Asia Pacific Science Press

Journal of Advances in Engineering and Technology
ISSN(O):3005-7507
ISSN(P):3005-7493
Vol. 2 No.4 (2025)

Construction of SnS_2/TiO_2 Heterojunction and Study of Its Photocatalytic Performance

Xiaofeng Zhang, Jinzhao Song*

School of Chemistry and Chemical Engineering, Ningxia University, 750021, China

Corresponding author: Jinzhao Song, 12024140163@stu.nxu.edu.cn

Abstract: This thesis primarily prepared SnS_2 and TiO_2 monomers, and subsequently fabricated SnS_2/TiO_2 composites via a one-step hydrothermal method using tetrabutyl titanate, anhydrous ethanol, and concentrated nitric acid. The morphologies of the two prepared monomers and the SnS_2/TiO_2 composite were characterized using scanning electron microscopy (SEM). The photocatalytic performance was evaluated by degrading methylene blue solution under xenon lamp irradiation. The results demonstrate that the SnS_2/TiO_2 composite exhibits excellent photocatalytic activity, achieving a degradation rate as high as 92% for the methylene blue dye.

Keywords: SnS_2/TiO_2 Composite; Photocatalysis; Hydrothermal Method; Methylene Blue

Published: Dec 17, 2025

DOI: https://doi.org/10.62177/jaet.v2i4.907

1.Introduction

In recent years, the continuous improvement in people's living standards and quality of life has been accompanied by increasingly severe environmental pollution, particularly water pollution.[1-2] For China, rapid population growth and the expansion of industrial and agricultural production have inevitably led to the generation of large quantities of various wastes during industrial processes. Concurrently, water pollution incidents frequently occur due to inadequate supervision, improper treatment measures, and weak public awareness of environmental protection. Industrial wastewater, waste residues, and exhaust gases have become major sources of water pollution. Although significant efforts have been made in water pollution control, the ongoing deterioration of the water environment has not yet been effectively curbed. Traditional chemical methods for treating water pollution are now on the verge of being phased out. Compared to traditional chemical reduction methods, semiconductor photocatalytic reduction technology offers distinct advantages for treating wastewater pollution.[3] Semiconductor photocatalysis is highly favored for dye degradation due to its efficiency and environmental friendliness.[4-5] The photocatalytic properties of a semiconductor are closely related to its band structure. When a semiconductor is irradiated with light whose photon energy is greater than or equal to its band gap energy ($h\upsilon \geq Eg$), the semiconductor absorbs the light energy, exciting electrons from the valence band to the conduction band and leaving behind an equal number of positively charged holes in the valence band.[6-7] The photogenerated electrons (e^-) possess strong reducing power, while the photogenerated holes (h^+) possess strong oxidizing power, together forming a highly active redox system. The specific photocatalytic principle is illustrated in Figure 1. TiO_2 is, to date, the most extensively studied and widely used semiconductor photocatalyst, exhibiting catalytic activity for numerous photochemical reactions, and is inexpensive and non-toxic. However, its relatively

large band gap energy (3.2 eV) means it can only be excited by ultraviolet light with $\lambda \leq 387.5$ nm, resulting in low utilization efficiency of solar energy, fast recombination of photogenerated electrons and holes, and low quantum efficiency. To make better use of solar energy, researchers worldwide have conducted extensive work in recent years on modifying TiO_2 and developing visible-light-responsive photocatalytic materials, achieving considerable progress.[8] Examples include non-metal element doping (e.g., S-TiO_2,[9] N-TiO_2), semiconductor composites (e.g., Cu_2O/TiO_2, Bi_2O_3/TiO_2,[10] $ZnMn_2O_4/TiO_2$ [11]), and new visible-light catalysts like $SnIn_4S_8$.[12] Among these, compositing TiO_2 with narrow-bandgap semiconductor materials has been a persistent research focus.SnS_2, an important semiconductor from the IV-VI group, has a band gap energy of 2.2 eV - 2.35 eV at room temperature.[13-14] While numerous studies based on existing literature have reported on the optical and electrical properties of SnS_2, there are relatively few publications concerning its photocatalytic properties. He, H.Y. et al. investigated the photocatalytic degradation of methyl orange in water by SnS_2/TiO_2 composites under natural sunlight, finding that the photocatalytic activity of the mixture increased with higher SnS_2 content.[15] Yang, C. et al. studied the photocatalytic performance of SnS_2/TiO_2 composites prepared via an in-situ chemical method, using methyl orange in water as the degradation target under visible and UV light.[16] The results showed that composites prepared by the in-situ method had higher photocatalytic activity than single components or physically mixed composites of the same composition, along with better photocatalytic stability.[17] Furthermore, Zhang, Y.C. et al. obtained SnS_2 nanosheets using a solid-liquid phase reaction from a mixture of $SnCl_2 \cdot 2H_2O$ and excess sulfur powder, and synthesized SnS_2 nanopowder via a simple hydrothermal method using $SnCl_4 \cdot 5H_2O$ and thioacetamide as raw materials.[18-19] They further prepared composite SnS_2/SnO nanopowder using an in-situ oxidation method. Evaluating the photocatalytic activity for methyl orange degradation under visible light or sunlight, they found that the synthesized SnS_2 or SnS_2/SnO composites exhibited high visible-light photocatalytic activity and stability. Based on the above research, this paper prepared SnS_2/TiO_2 composites via a one-step hydrothermal method.[20] The morphology of the synthesized SnS_2/TiO_2 composites was observed using scanning electron microscopy, and their photocatalytic performance was investigated by degrading methylene blue solution under xenon lamp irradiation.

2.Material Preparation

2.1 Preparation of TiO_2 Powder

First, prepare two 50 mL beakers. Precisely measure 900 μL of absolute ethanol and tetrabutyl titanate separately using a pipette gun, pour them into one beaker, and mix thoroughly with a magnetic stirrer. Label this as Solution A. Then, measure 4.5 mL of deionized water using a pipette gun and pour it into the other 50 mL beaker. Add 25 μL of concentrated nitric acid to the deionized water using the pipette gun, and mix thoroughly with a magnetic stirrer. Label this as Solution B. Gradually add Solution A dropwise into Solution B to obtain the precursor solution of tetrabutyl titanate. Transfer the entire precursor solution into a 25 mL polytetrafluoroethylene-lined stainless steel hydrothermal autoclave. Place the autoclave in an oven set at 160°C for 6 hours. After the reaction is complete and the autoclave has cooled naturally to room temperature, open it. Use a pipette to remove the supernatant from the liner. Wash the precipitate once with deionized water and centrifuge, discarding the supernatant. Then wash the precipitate twice with absolute ethanol, centrifuge, and collect the precipitate. Place the precipitate in an oven set at 60°C for 1 hour to dry. Transfer the dried precipitate into a crucible and place it in a muffle furnace. Set the calcination temperature to 500°C with a heating rate of 5°C/min, and calcine for 2 hours to obtain TiO_2 powder. Grind the powder for later use.

2.2 Preparation of SnS_2 Nanomaterials

Weigh 0.3502 g of tin(IV) chloride pentahydrate, 0.3024 g of thioacetamide, and 0.3031 g of citric acid separately using an analytical balance. Transfer all the weighed chemicals into a 100 mL beaker, add 10 mL of absolute ethanol, and stir with a magnetic stirrer until fully dissolved. Transfer the entire solution into a 25 mL polytetrafluoroethylene-lined stainless steel hydrothermal autoclave. Place the autoclave in an oven set at 180°C for 12 hours. After the reaction is complete and the autoclave has cooled naturally to room temperature, open it. Remove the supernatant using a pipette. Wash the precipitate once with deionized water and centrifuge, then discard the supernatant. Repeat the washing process twice with absolute ethanol, centrifuging each time and discarding the supernatant. Collect the precipitate and place it in an oven set at 80°C for 6 hours to

dry. The final product is the prepared SnS_2 material, which should be ground for later use.

2.3 Preparation of SnS_2/TiO_2 Composite Material

Weigh 1.0520 g of tin(IV) chloride pentahydrate and 0.5635 g of thioacetamide using an analytical balance, and sequentially add them into a mixed solution containing 30.0 mL of absolute ethanol and 2.0 mL of glacial acetic acid. Stir continuously for 10 minutes to form a transparent solution. Add 256 μL of tetrabutyl titanate solution to the above mixture using a pipette gun and mix thoroughly with a magnetic stirrer. Transfer the resulting solution into a 50 mL polytetrafluoroethylene-lined stainless steel hydrothermal autoclave. Place the autoclave in an oven set at 160°C for 12 hours. After the reaction is complete and the autoclave has cooled to room temperature, open it. Remove the supernatant using a pipette. Wash the precipitate once with deionized water, centrifuge, and discard the supernatant. Then wash the precipitate twice with absolute ethanol, centrifuge, and collect the precipitate. Place the precipitate in an oven set at 60°C and dry for 5 hours to obtain the SnS_2/TiO_2 composite material. Grind the product for later use.

3.Surface Morphology Analysis

Figure1: SEM image of TiO_2

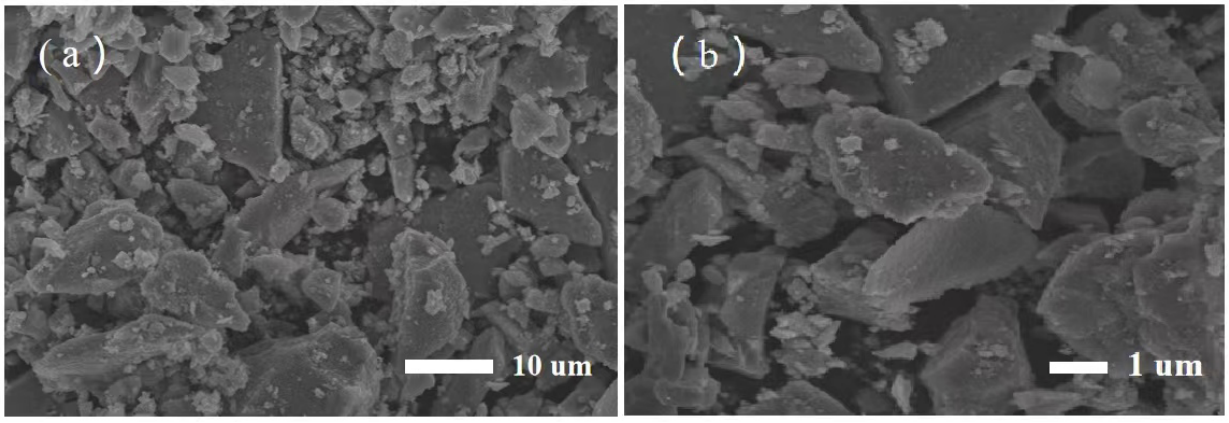

Figure 1 shows scanning electron microscopy (SEM) images of TiO_2 at different magnifications. The images reveal that the cross-sectional diameter of the material is approximately 10 μm. Additionally, TiO_2 exhibits an irregular morphology, with two-dimensional TiO_2 particles aggregating to form plate-like structures, and the grain size is relatively large.

Infrastructure Construction Cost for Reverse Logistics: This refers to the expenses required for building the fundamental facilities necessary for the normal operation of the reverse logistics network. These facilities include collection points, transfer stations, processing centers, waste incineration plants, and landfills.

Figure2: SEM images of SnS_2

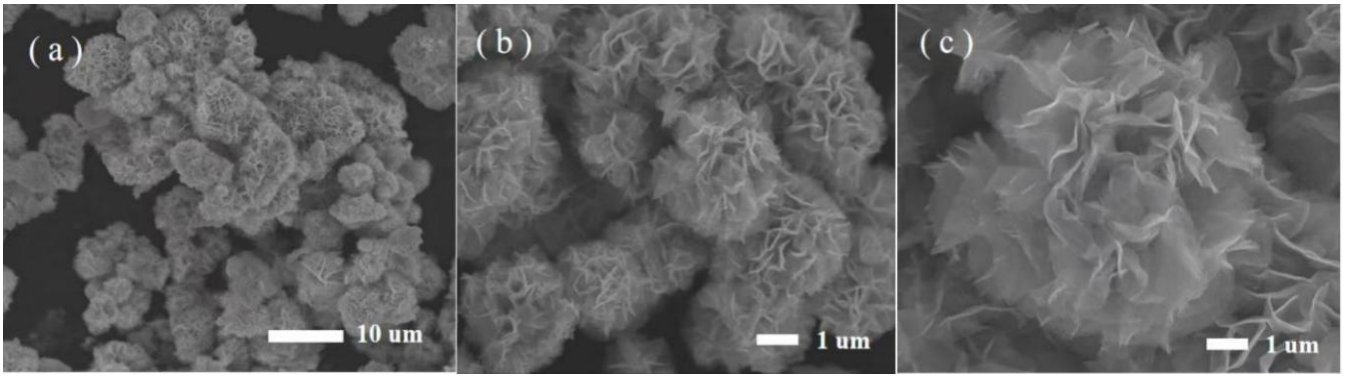

Figure 2 displays scanning electron microscopy (SEM) images of SnS_2 at different magnifications.It can be clearly observed that SnS_2 exhibits a flower-like structure composed of stacked two-dimensional nanosheets. These flower-like structures are well-dispersed, with a diameter of approximately 3 μm. Additionally, the rough surface texture and distinct morphological features of the material are clearly visible.

Figure3: SEM images of SnS_2/TiO_2 composite material

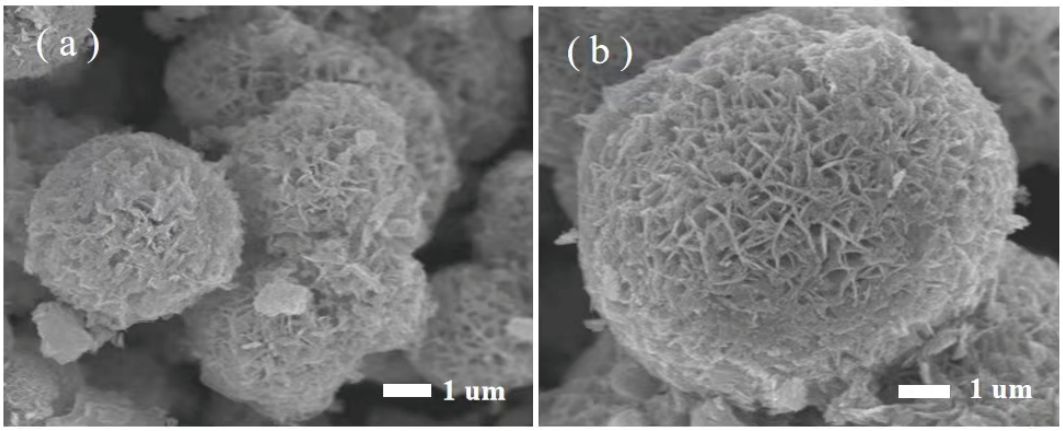

Figure 3 shows the scanning electron microscopy (SEM) images of the composite material. The images reveal that the SnS_2/TiO_2 composite, prepared via the hydrothermal method, exhibits a morphology intermediate between the two individual components, with a diameter of approximately 4–5 μm. TiO_2 is uniformly dispersed within SnS_2, making it difficult to distinguish individual particles. In the composite material, SnS_2 is encapsulated by TiO_2, which mitigates the morphological defects of both individual components. While the overall morphology of the composite remains largely consistent with that of SnS_2, noticeable aggregation occurs in the composite, contrasting with the dispersed flower-like structure of pure SnS_2.

4.Study of Photocatalytic Performance

First, a methylene blue solution with a concentration of 20 mg/L was prepared: 10 mg of methylene blue was weighed using an analytical balance, placed in a beaker, dissolved with an appropriate amount of deionized water, and then transferred to a 500 mL volumetric flask. Deionized water was added to the flask to bring the volume to the 500 mL mark, and the solution was mixed thoroughly for later use. Subsequently, 10 mg each of TiO_2, SnS_2, and SnS_2/TiO_2 composite material, ground using an agate mortar, were weighed and set aside.

4.1 Determination of Maximum Absorption Wavelength

Two clean Petri dishes were prepared, and 20 mL of the prepared 20 mg/L methylene blue solution was measured into each using a graduated cylinder. To one of the dishes, 10 mg of the SnS_2/TiO_2 composite material was added, while the other dish was used as a control. Both dishes were placed 20 cm below the light outlet of a xenon lamp and irradiated. Samples were taken every 5 minutes. For the dish containing the composite material, centrifugation was performed prior to sampling. The absorbance of each sample was measured using a UV-Vis spectrophotometer, and the data were recorded and plotted.

Figure4: Absorbance at Different Wavelengths

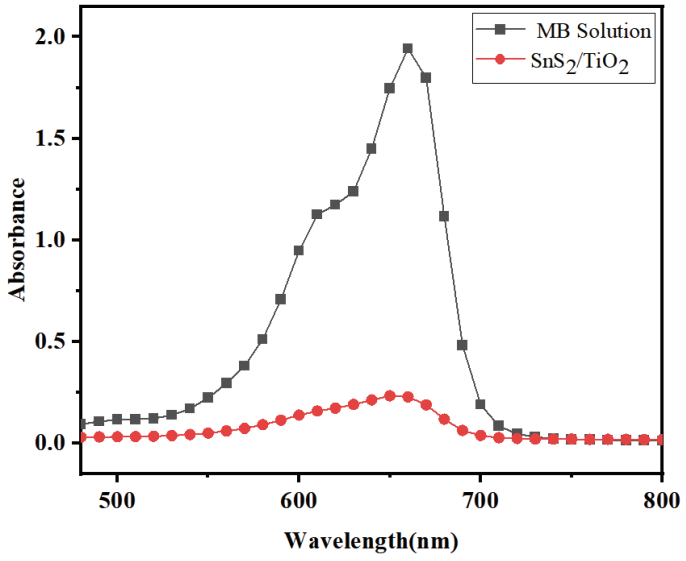

As shown in Figure 4, the maximum absorption wavelength of the 20 mg/L methylene blue solution is 664 nm. Over time, the absorbance of the methylene blue solution decreases significantly due to the addition of the SnS_2/TiO_2 composite material. This is reflected in the graph by the red curve consistently lying below the black curve, with the most pronounced reduction in absorbance observed at the maximum absorption wavelength.

4.2 Study on the Photocatalytic Performance of TiO_2, SnS_2, and SnS_2/TiO_2

A baseline was first established by scanning an appropriate amount of deionized water in a cuvette using a UV-Vis spectrophotometer. Another cuvette was filled with a prepared 20 mg/L methylene blue solution and scanned as Sample 1. Then, 10 mg of the pre-weighed TiO_2 powder was dissolved in a Petri dish containing 20 mL of the 20 mg/L methylene blue dye solution. The Petri dish was placed 20 cm below the light outlet of a xenon lamp for irradiation. Every 5 minutes, a 3 mL sample was taken, centrifuged, and the supernatant was transferred to a cuvette to measure its absorbance using the UV-Vis spectrophotometer. This experimental procedure was repeated six times, and changes in the color of the methylene blue dye were observed. After completing the six sets of experiments with TiO_2, the Petri dish and cuvette were washed with deionized water and absolute ethanol, then dried. The TiO_2 powder in the Petri dish was replaced with the pre-ground SnS_2 powder and SnS_2/TiO_2 powder, respectively, and the above experimental steps were repeated for each material. Changes in the color of the methylene blue dye were observed accordingly.

Figure5: Absorbance of Methylene Blue Solution Degraded by Different Samples (a) Pure methylene blue solution; (b) TiO_2; (c) SnS_2; (d) SnS_2/TiO_2 composite material

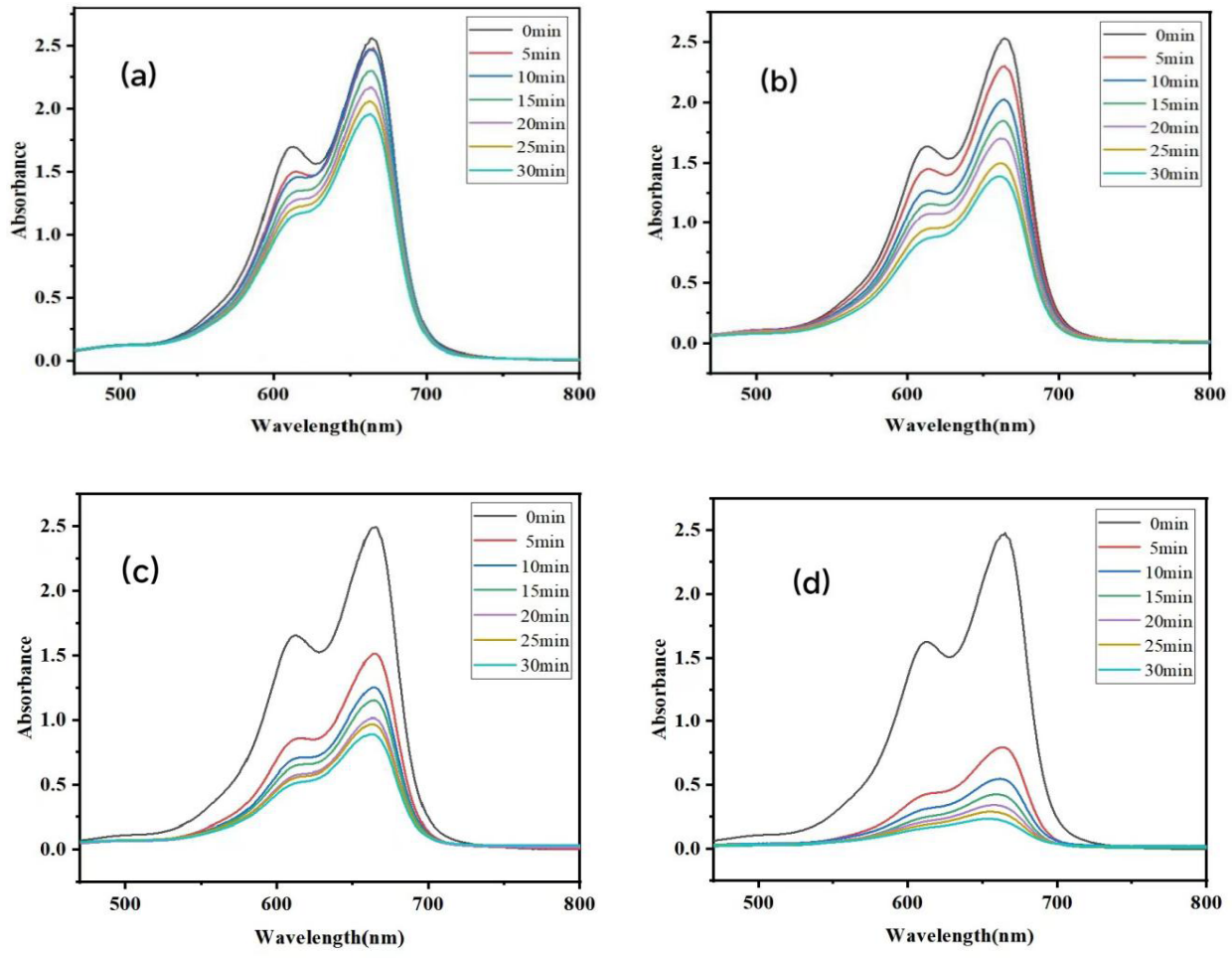

In Figure 5, the horizontal axis represents the wavelength, and the vertical axis represents the absorbance of each material. From Figure 5(a), it can be observed that the pure methylene blue solution without any catalyst exhibits the highest absorbance at all time intervals, with negligible changes in absorbance over time. Figures 5(b), (c), and (d) show that the absorbance of the solution decreases significantly after the addition of different catalysts compared to the pure methylene blue

solution. The methylene blue solution with SnS_2 added shows the second most significant reduction in absorbance after the SnS_2/TiO_2 composite. Furthermore, Figure (b) indicates that TiO_2 has a less pronounced effect on reducing the absorbance of the methylene blue solution compared to SnS_2 and the composite material. Additionally, it is observed that as time increases, the reduction in absorbance of the methylene blue solution by TiO_2, SnS_2, and the SnS_2/TiO_2 composite becomes more pronounced. Comparing the four graphs, it is evident that the SnS_2/TiO_2 composite material (Figure d) achieves the most effective reduction in absorbance of the methylene blue solution.

4.3 Study of Degradation Performance

The absorbance data of the pure methylene blue solution and the methylene blue solutions with added TiO_2, SnS_2, and SnS_2/TiO_2 composite, respectively, were processed to obtain the following figure.

Figure6: Degradation curves of methylene blue solutions with different materials added

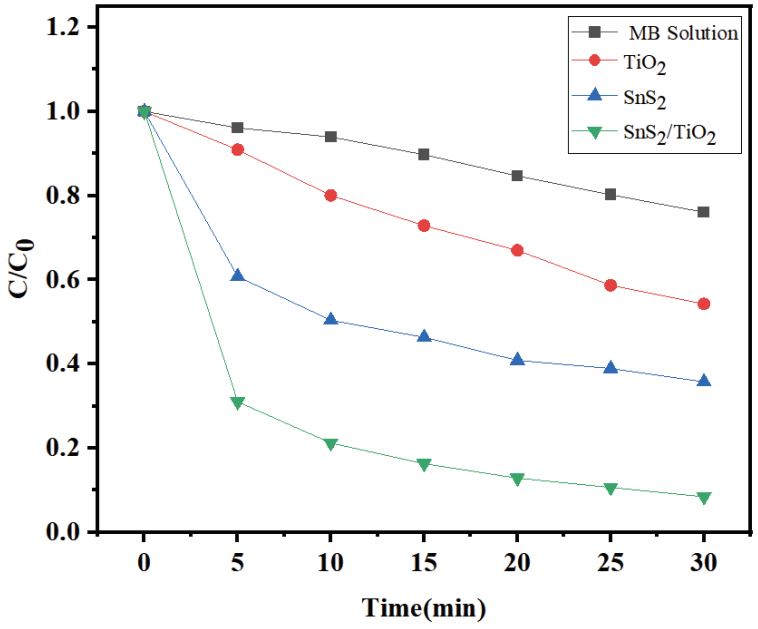

From Figure 6, it can be observed that under the same degradation time, the pure methylene blue solution without any photocatalyst shows negligible degradation, with a degradation rate of only 24% after 30 minutes. In contrast, the degradation efficiency of methylene blue solutions with different photocatalysts added is significantly improved. The red dotted curve exhibits a degradation rate of approximately 46% after 30 minutes, which is 1.9 times higher than that of the pure methylene blue solution. The blue triangular curve achieves a degradation rate of about 65% after 30 minutes, representing a 2.7-fold increase compared to the pure methylene blue solution. The green curve demonstrates the best degradation performance, reaching a degradation rate of 92% after 30 minutes, which is 3.8 times higher than that of the pure methylene blue solution. Therefore, it can be concluded that the SnS_2/TiO_2 composite material exhibits the most effective degradation of methylene blue solution, with the highest dye degradation rate.

Conclusion

The main focus of this study was the preparation of SnS_2/TiO_2 composite material via a one-step hydrothermal method, followed by morphological characterization, absorbance measurement, and investigation of its photocatalytic performance. The following key findings were obtained:

1.The maximum absorption wavelength of the SnS_2/TiO_2 composite material for methylene blue solution was determined to be 664 nm.

2.The degradation efficiency of pure methylene blue solution without any photocatalyst was negligible, while the addition of different photocatalysts significantly enhanced the degradation performance.

3.Under controlled conditions with identical degradation time, light intensity, and material dosage, the SnS_2/TiO_2 composite material achieved the highest degradation efficiency of 92% for methylene blue solution. This indicates that the photocatalytic

performance of the composite is superior to that of its individual components.

4.The composite material prepared by the hydrothermal method demonstrates promising potential for applications in the field of photocatalysis, fulfilling the objectives and expectations of this study.

Funding

No

Conflict of Interests

The authors declare that there is no conflict of interest regarding the publication of this paper.

Reference

[1] Guo, C. B. (2021). Two-dimensional bismuth selenide anchored semiconductor catalyst and its photocatalytic performance [Doctoral dissertation]. Xiangtan University. https://doi.org/10.27426/d.cnki.gxtdu.2021.000555

[2] Xu, B. X., & Yuan, F. (2011). Where is the water of life (pp. 8–9, 105–117). Beijing Yanshan Press.

[3] Zhou, X. L. (2011). Chemistry and daily life (pp. 18–26). China Electric Power Press.

[4] Wang, B., Zhang, X., Zhang, N., et al. (2015). Two-dimensional MoS_2 nanosheet-coated Bi_2S_3 discoids: Synthesis, formation mechanism, and photocatalytic application. Langmuir, 31(14), 4314–4322. https://doi.org/10.1021/acs.langmuir.5b00544

[5] He, H. Y., Huang, J. F., Cao, L. Y., & Wu, J. P. (2007). Photocatalytic activity of mixture of SnS_2 and TiO_2 powders in destruction of methyl orange in water. Optoelectronic Advanced Materials, 12, 3781–3784. https://doi.org/10.1166/oam.2007.1452

[6] Humayun, M., Raziq, F., Khan, A., et al. (2018). Modification strategies of TiO_2 for potential applications in photocatalysis: A critical review. Green Chemistry Letters and Reviews, 11(2), 86–102. https://doi.org/10.1080/17518253.2017.1366786

[7] Zhang, Y. C., Du, Z. N., Li, S. Y., & Zhang, M. (2010). Novel synthesis and high visible light photocatalytic activity of SnS_2 nanoflakes from $SnCl_2{\cdot}2H_2O$ and S powders. Applied Catalysis B: Environmental, 95, 153–159. https://doi.org/10.1016/j.apcatb.2009.11.015

[8] Akpan, U. G., & Hameed, B. H. (2009). Parameters affecting the photocatalytic degradation of dyes using TiO_2-based photocatalysts: A review. Journal of Hazardous Materials, 170, 520–529. https://doi.org/10.1016/j.jhazmat.2009.06.002

[9] Zheng, L. X., et al. (2020). Photo/electro chemical applications of metal sulfide/TiO_2 heterostructures. Advanced Energy Materials, 10(1), 1902355. https://doi.org/10.1002/aenm.201902355

[10] Kumair, et al. (2016). Efficiency enhancement in plasmonic dye-sensitized solar cells with TiO_2 photoanodes incorporating gold and silver nanoparticles. Journal of Applied Electrochemistry, 46(1), 47–58. https://doi.org/10.1007/s10800-015-0944-8

[11] Wang, J., & Zhuan, R. (2020). Degradation of antibiotics by advanced oxidation processes: An overview. Science of the Total Environment, 701, 135023. https://doi.org/10.1016/j.scitotenv.2019.135023

[12] Wei, Z., Liu, J., & Shangguan, W. (2020). A review on photocatalysis in antibiotic wastewater: Pollutant degradation and hydrogen production. Chinese Journal of Catalysis, 41(10), 1440–1455. https://doi.org/10.1016/S1872-2067(20)63698-8

[13] Kovalakova, P., Cizmas, L., McDonald, T. J., et al. (2020). Occurrence and toxicity of antibiotics in the aquatic environment: A review. Chemosphere, 251, 126351. https://doi.org/10.1016/j.chemosphere.2020.126351

[14] Martinez, J. L. (2009). Environmental pollution by antibiotics and by antibiotic resistance determinants. Environmental Pollution, 157(11), 2893–2902. https://doi.org/10.1016/j.envpol.2009.07.031

[15] Yang, C., Wang, W., Shan, Z., & Huang, F. (2009). Preparation and photocatalytic activity of high-efficiency visible-light-responsive photocatalyst SnS_2/TiO_2. Solid State Chemistry, 182, 807–812. https://doi.org/10.1016/j.solidstatesciences.2009.02.016

[16] Ismail, A. A., & Bahnemann, D. W. (2014). Photochemical splitting of water for hydrogen production by photocatalysis: A review. Solar Energy Materials and Solar Cells, 128, 85–101. https://doi.org/10.1016/j.solmat.2014.03.034

[17] Wang, J., Wang, J., Wu, X., et al. (2017). Pt-TiO_2 microspheres with exposed {001} facets for degradation of formaldehyde in air: Formation mechanism and enhanced visible light photocatalytic activity. Materials Research Bulletin, 96, 262–269. https://doi.org/10.1016/j.materresbull.2017.08.031

[18] Zhang, Y. C., Du, Z. N., Li, K. W., et al. (2011). Size-controlled hydrothermal synthesis of SnS_2 nanoparticles with high performance in visible light-driven photocatalytic degradation of aqueous methyl orange. Separation and Purification Technology, 81(1), 101–107. https://doi.org/10.1016/j.seppur.2011.06.018

[19] Reli, M., Huo, P., Sihor, M., et al. (2016). Novel TiO_2/C_3N_4 photocatalysts for photocatalytic reduction of CO_2 and for photocatalytic decomposition of N_2O. Journal of Physical Chemistry A, 120(43), 8564–8573. https://doi.org/10.1021/acs.jpca.6b08444

[20] Anucha, C. B., Altin, I., Bacaksiz, E., et al. (2022). Titanium dioxide (TiO_2)-based photocatalyst materials activity enhancement for contaminants of emerging concern (CECs) degradation: In the light of modification strategies. Chemical Engineering Journal Advances, 10, 100262. https://doi.org/10.1016/j.ceja.2022.100262